Temperature Effects on the Catalytic Activity of the D38E Mutant of 3-Oxo-Δ⁵-Steroid Isomerase: Favorable Enthalpies and Entropies of Activation Relative to the Nonenzymatic Reaction Catalyzed by Acetate Ion

Wendy J. Houck and Ralph M. Pollack*

Contribution from the Department of Chemistry and Biochemistry, University of Maryland, Baltimore County, 1000 Hilltop Circle, Baltimore, Maryland 21250

Received May 28, 2004; E-mail: pollack@umbc.edu

Abstract: 3-Oxo-Δ⁵-steroid isomerase (ketosteroid isomerase, KSI) catalyzes the isomerization of 5-androstene-3,17-dione (**1**) to 4-androstene-3,17-dione (**3**) via a dienolate intermediate (**2⁻**). KSI catalyzes this conversion about 13 orders of magnitude faster than the corresponding reaction catalyzed by acetate ion, a difference in activation energy ($\Delta G^{\ddagger}$) of ~18 kcal/mol. To evaluate whether the decrease in $\Delta G^{\ddagger}$ by KSI is due to enthalpic or entropic effects, the activation parameters for the isomerization of **1** catalyzed by the D38E mutant of KSI were determined. A linear Arrhenius plot of k_{cat}/K_M versus $1/T$ gives the activation enthalpy ($\Delta H^{\ddagger} = 5.9$ kcal/mol) and activation entropy ($T\Delta S^{\ddagger} = -2.6$ kcal/mol). Relative to catalysis by acetate, D38E reduces $\Delta H^{\ddagger}$ by ~10 kcal/mol and increases $T\Delta S^{\ddagger}$ by ~5 kcal/mol. The activation parameters for the microscopic rate constants for D38E catalysis were also determined and compared to those for the acetate ion-catalyzed reaction. Enthalpic stabilization of **2⁻** and favorable entropic effects in both chemical transition states by D38E result in an overall energetically more favorable enzymatic reaction relative to that catalyzed by acetate ion.

Introduction

Enzymes are able to enhance the rate of chemical reactions by as much as 23 orders of magnitude.[1] The dramatic effects of enzymes on reaction rates have been postulated to arise from a variety of factors, such as orbital steering,[2-4] stereopopulation control,[5] near attack conformations (NACs),[6] chelation effects,[7] strain–distortion,[8] transition-state stabilization,[9-13] substrate destabilization,[7] and preorganization of the active site.[14] Alternatively, one may wish to assess the enthalpic and entropic contributions to catalysis inherent in enzyme reactions relative to those in solution reactions. Generally, enthalpic contributions arise predominantly from ionic and polar interactions, whereas entropic contributions arise from solvation changes to an enzyme and/or substrate and reorganization of the active site.[7] Comparison of the activation parameters of the enzymatic reaction to the corresponding nonenzymatic reaction enables a unique assessment of the specific forces driving enzyme catalysis. It has generally been found that enzymes function by their ability to drastically reduce the enthalpy of activation ($\Delta H^{\ddagger}$) while only minimally affecting the entropy of activation ($T\Delta S^{\ddagger}$).[15-20]

There are several enzymes for which the activation enthalpies and entropies have been determined. A comparison of the enzymatic rate constant, k_{cat}, to the rate constant for the corresponding nonenzymatic reaction, k_{non}, shows moderate to drastic reductions in the activation enthalpy with chorismate mutase ($\Delta\Delta H^{\ddagger} = 9$ kcal/mol),[20] mandelate racemase ($\Delta\Delta H^{\ddagger} = 15.5$ kcal/mol),[19] and yeast OMP decarboxylase ($\Delta\Delta H^{\ddagger} = 33.4$ kcal/mol).[15] Since these and other enzymes[15] effect little to no changes in the activation entropy, the reduction in enthalpy is the driving force in such enzymatic reactions. Notably though, there are a few instances in which an enzyme increases the entropy of activation, contributing several orders of magnitude to the enzymatic rate acceleration. For example, deamination of 5,6-dihydrocytidine by cytidine deaminase is ~8 kcal/mol entropically more favorable than the corresponding non-enzymatic deamination, with no change in the activation enthalpy.[18]

(1) Radzicka, A.; Wolfenden, R. *Science* **1995**, *267*, 90.
(2) Dafforn, A.; Koshland, D. E., Jr. *Biochem. Biophys. Res. Commun.* **1973**, *52*, 779.
(3) Dafforn, A.; Koshland, D. E., Jr. *Proc. Natl. Acad. Sci. U.S.A.* **1971**, *68*, 2463.
(4) Page, M. I.; Jencks, W. P. *Biochem. Biophys. Res. Commun.* **1974**, *57*, 887.
(5) Milstien, S.; Cohen, L. A. *Proc. Natl. Acad. Sci. U.S.A.* **1970**, *67*, 1143.
(6) Bruice, T. C. *Acc. Chem. Res.* **2002**, *35*, 139.
(7) Jencks, W. P. *Adv. Enzymol. Relat. Areas Mol. Biol.* **1975**, *43*, 219.
(8) Jencks, W. P. *Catalysis in Chemistry and Enzymology*; Dover Publications: New York, 1987; p 282.
(9) Lienhard, G. E. *Science* **1973**, *180*, 149.
(10) Wolfenden, R. *Acc. Chem. Res.* **1972**, *5*, 10.
(11) Kraut, J. *Science* **1988**, *242*, 533.
(12) Warshel, A.; Štrajbl, M.; Villá, J.; Florián, J. *Biochemistry* **2000**, *39*, 14728.
(13) Villá, J.; Štrajbl, M.; Glennon, T. M.; Sham, Y. Y.; Chu, Z. T.; Warshel, A. *Proc. Natl. Acad. Sci. U.S.A.* **2000**, *97*, 11899.
(14) Warshel, A. *J. Biol. Chem.* **1998**, *273*, 27035.
(15) Wolfenden, R.; Snider, M.; Ridgway, C. Miller, B. *J. Am. Chem. Soc.* **1999**, *121*, 7419.
(16) Eftink, M. R.; Biltonen, R. L. *Biochemistry* **1983**, *22*, 5140.
(17) Snider, M. J.; Gaunitz, S.; Ridgway, C.; Short, S. A.; Wolfenden, R. *Biochemistry* **2000**, *39*, 9746.
(18) Snider, M. J.; Lazarevic, D.; Wolfenden, R. *Biochemistry* **2002**, *41*, 3925.
(19) St. Maurice, M.; Bearne, S. L. *Biochemistry* **2002**, *41*, 4048.
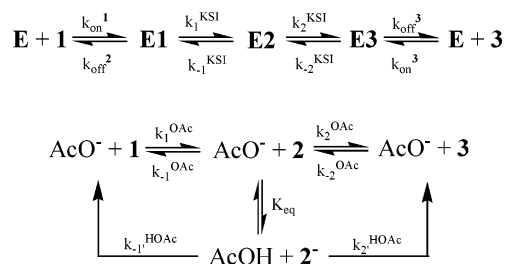(20) Andrews, P. R.; Smith, G. D.; Young, I. G. *Biochemistry* **1973**, *12*, 3492.

Scheme 1
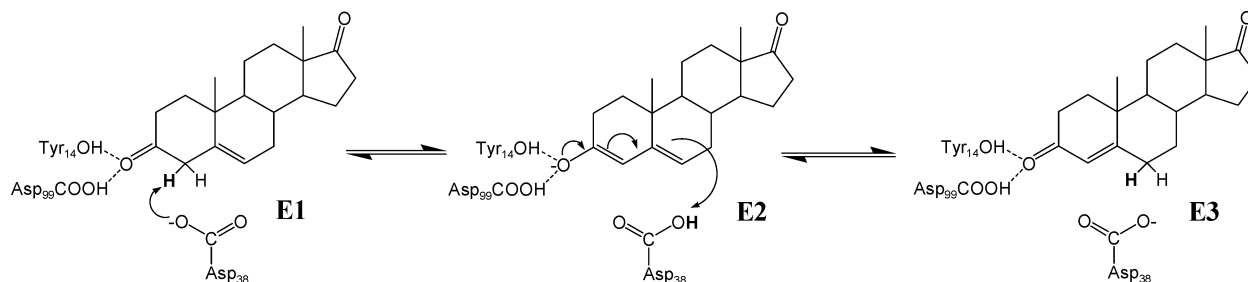
To better understand enthalpic and entropic contributions to enzyme catalysis, it is instructive to compare an enzymatic reaction to the same reaction catalyzed by a model compound, thereby enabling the determination of the function of "the rest of the enzyme" in catalysis. This approach requires that the mechanisms for the enzymatic reaction and the nonenzymatic model reaction be similar and that both be known in sufficient detail so that the individual steps of catalysis can be compared. In complicated mechanisms, particularly one in which there is more than one rate-determining step, it is difficult to attribute overall changes in entropy and enthalpy (k_{non}, k_{cat}, or k_{cat}/K_M) to specific mechanistic details. However, a comparison of the entropic and enthalpic activation parameters for the individual steps of enzymatic and nonenzymatic reactions could lead to an analysis of catalysis in terms of specific changes in chemical structure, electrostatic interactions, and solvation. This report describes the determination of the activation parameters for the microscopic rate constants of the isomerization of 5-androstene-3,17-dione (**1**) to 4-androstene-3,17-dione (**3**) catalyzed by 3-oxo-Δ⁵-steroid isomerase (ketosteroid isomerase, KSI) and a comparison of these parameters to the activation parameters for the nonenzymatic reaction catalyzed by an acetate ion.[21]

KSI has been studied extensively by us and by others,[22−36] and significant mechanistic detail is known. KSI catalyzes the isomerization of **1** to its conjugated isomer **3** through a dienolate intermediate at a rate near the diffusion-controlled limit.[26] Although there was some initial disagreement,[37] the mechanism of Scheme 1 is now generally agreed upon.[19,33,35] This mechanism involves an initial proton abstraction from C-4 of **1** by the active site base, Asp38, to give a negatively charged oxyanion (**2⁻**), which is stabilized by hydrogen bonds between

(21) Houck, W. J.; Pollack, R. M. *J. Am. Chem. Soc.* **2003**, *125*, 10206.
(22) Talalay, P.; Wang, V. S. *Biochim. Biophys. Acta* **1955**, *18*, 300.
(23) Benisek, W. F.; Ogez, J. R.; Smith, S. B. *Ann. N. Y. Acad. Sci.* **1980**, *346*, 115.
(24) Kuliopolis, A.; Mildvan, A. S.; Shortle, D.; Talalay, P. *Biochemistry* **1989**, *28*, 149.
(25) Eames, T. C. M.; Pollack, R. M.; Steiner, R. F. *Biochemistry* **1989**, *28*, 6269.
(26) Hawkinson, D. C.; Eames, T. C. M.; Pollack, R. M. *Biochemistry* **1991**, *30*, 10849.
(27) Zeng, B.; Pollack, R. M. *J. Am. Chem. Soc.* **1991**, *113*, 3838.
(28) Wu, Z. R.; Ebrahimian, S.; Zawrotny, M. E.; Thornburg, L. D.; Perez-Alvarado, G. C.; Brothers, P.; Pollack, R. M.; Summers, M. F. *Science* **1997**, *276*, 415.
(29) Thornburg, L. D.; Hénot, F.; Bash, D. P.; Hawkinson, D. C.; Bartel, S. D.; Pollack, R. M. *Biochemistry* **1998**, *37*, 10499.
(30) Cho, H.-S.; Ha, N.-C.; Choi, G.; Kim, H.-J.; Lee, D.; Oh, K. S.; Kim, K. S.; Lee, W.; Choi, K. Y.; Oh, B.-H. *J. Biol. Chem.* **1999**, *274*, 32863.
(31) Pollack, R. M.; Thornburg, L. D.; Wu, Z. R.; Summers, M. F. *Arch. Biochem. Biophys.* **1999**, *370*, 9.
(32) Thornburg, L. D.; Goldfeder, Y. R.; Wilde, T. C.; Pollack, R. M. *J. Am. Chem. Soc.* **2001**, *123*, 9912.
(33) Feierberg, I.; Åqvist, J. *Biochemistry* **2002**, *41*, 15728.
(34) Park, H.; Merz, K. M., Jr. *J. Am. Chem. Soc.* **2003**, *125*, 901.
(35) Mazumder, D.; Kahn, K.; Bruice, T. C. *J. Am. Chem. Soc.* **2003**, *125*, 7553.
(36) Yun, Y. S.; Lee, T. H.; Nam, G. H.; Jang, do S.; Shin, S.; Oh, B. H.; Choi, K. Y. *J. Biol. Chem.* **2003**, *278*, 28229.

Scheme 2

it and both Tyr14 and Asp99.[24,29] Subsequent reprotonation at C-6 by Asp38 results in the conjugated product. The isomerization of **1** is also catalyzed by acetate through a similar mechanism, although at a much slower rate.[21,27] Microscopic rate constants for both KSI- and acetate-catalyzed isomerization (Scheme 2) have been determined, and free energy profiles for the complete reactions have been characterized.[26,27]
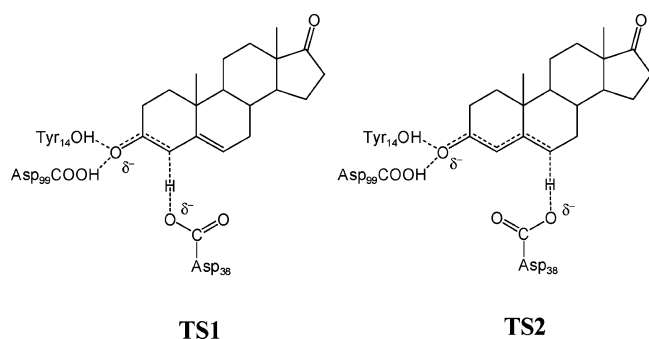
A comparison of the free energy profiles of KSI-catalyzed and acetate-catalyzed isomerization shows important differences between the two reactions (Figure 1). In the nonenzymatic reaction, the intermediate partitions back to reactant ∼50-fold more often than it proceeds to product (corresponding to a $\Delta\Delta G^{\ddagger}$ of ∼2 kcal/mol).[21,27] In the enzymatic reaction, however, the
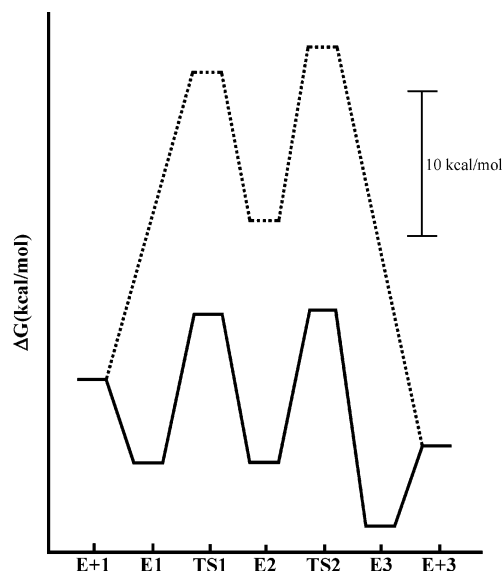
Figure 1. Free energy diagram for isomerization of **1** to **3** catalyzed by WT (−) and by acetate ion (· · ·), based on previously determined rate constants at 25.0 °C.[26,27] Enzymatic conversions are first order (s⁻¹), and acetate ion-catalyzed conversions are second order (M⁻¹ s⁻¹). The *x*-axis corresponds to the reaction coordinate for KSI-catalyzed isomerization. The corresponding acetate ion-catalyzed mechanism is AcO⁻ + **1** ⇌ **TS1ᴬᶜ** ⇌ AcOH + **2⁻** ⇌ **TS2ᴬᶜ** ⇌ AcO⁻ + **3**. Barriers due to **E** + **1** association/dissociation and barriers due to acetate-catalyzed rate constants assume a standard state of 1 M.

Scheme 3

rate constants for partitioning of the intermediate ($k_{-1}{}^{KSI}$ and $k_2{}^{KSI}$) are almost identical, leading to a partitioning ratio ($k_{-1}{}^{KSI}/k_2{}^{KSI}$) of about three ($\Delta\Delta G^{\ddagger} \sim 0.6$ kcal/mol).[26] Thus, the relative energies of the two chemical transition states for interconversion of **E1** ⇌ **E2** and **E2** ⇌ **E3** (**TS1** and **TS2**, respectively) are about the same for KSI catalysis but quite different for acetate ion catalysis. The ability of KSI to isomerize **1** ~13 orders of magnitude faster than does acetate[26,27] can be attributed to (1) the stabilization of the enzyme-bound intermediate and flanking transition states by >10 orders of magnitude[26] and (2) the ability of KSI to discriminate between the two chemical transition states.[32] It is unclear how KSI is able to discriminate between these two seemingly similar chemical transition states (Scheme 3), and the specific factors governing both substrate and intermediate binding are unknown.

We have previously determined the activation parameters for the acetate-catalyzed isomerization of **1** to **3** and found that, generally, the microscopic rate constants are both enthalpically and entropically costly.[21] The present work resolves the microscopic rate constants for the D38E mutant of KSI into their enthalpic and entropic contributions to the overall free energy. We use the D38E mutant of KSI because the activity of the wild-type enzyme is partly diffusion controlled, making a detailed evaluation of the temperature-dependent reaction kinetics difficult. However, only chemical steps contribute to the reaction rate for D38E, although this mutant still has significant catalytic activity (k_{cat}/K_M and k_{cat} are only ~300- and 200-fold less than that of the wild type, respectively).[38] The carboxylate functionality is retained upon mutation of Asp to Glu, and the free energy profile of D38E has also been characterized, allowing a determination of the microscopic rate constants.[38] As with WT, there is no single rate-determining step for D38E, and the partitioning ratio of **2**⁻ by D38E is near unity.

Materials and Methods

Materials. 5-Androstene-3,17-dione was prepared by G. Blotny of this laboratory according to a previously published procedure.[39] Buffers and hydroxide solutions were prepared with reagent-grade chemicals or better. Buffer pH was determined on a Radiometer PHM85 Precision pH meter and is within 0.1 units of the values given throughout the text. For all of the kinetic experiments, solutions were thermostated for at least 15 min so that constant temperature was maintained prior to commencing a run.

Cloning, Expression, and Purification of D38E. Preparation of the D38E mutant of KSI is based on a combination of published procedures[29,40] and is summarized below. The pKSI$_{tac}$ vector, which contains the KSI gene,[41] and two primers designed to introduce the D38E mutation, 5′-GCCACGGTGGAAGAACCCTGTGGTTCCG-3′ and 5′-CGGTGCCACCTTCTTGGGCACCCAAGGC-3′, were used to prepare the mutant D38E−KSI. PCR reactions were carried out in a PTC-100 Programmable Thermocycler (MJ Research) according to the following protocol: step 1, 0.5 min at 95 °C; step 2, 1.0 min at 55 °C; step 3, 6.0 min at 70 °C for 16 cycles, preceded by an initial melting period of 1 min at 95 °C, according to guidelines in Stratagene's QuickChange Site-Directed Mutagenesis Kit. Recombinant vectors were transformed into XL2-Blue Ultracompetent *Escherichia coli* cells (Stratagene) and selected by ampicillin resistance. Plasmid DNA was purified using a QIAprep Spin Miniprep Kit (Qiagen) and was sequenced by the Biopolymer Laboratory at the University of Maryland, Baltimore.

Cells were grown in 100 mL of LB medium (100 μg/mL of ampicillin) for 16 h at 37 °C with shaking (200 rpm) and then were transferred to 2 L of LB medium (0.5 μM IPTG and 100 μg/mL of ampicillin) and grown for an additional 20 h at the same conditions. Harvested cells were pelleted by centrifugation and disrupted by BugBuster Protein Extraction Reagent (Novagen). The resultant mixture was centrifuged again to remove debris, and soluble protein was precipitated by dropwise addition of a solution of 95% ethanol and MgCl$_2$ (final concentrations were 80% ethanol, 5mM MgCl$_2$). This mixture was stirred for an additional hour after precipitation and was left at 4 °C overnight. The precipitate was recovered by centrifugation and resuspended in 10 mM Tris phosphate buffer (pH 7.0). After another centrifugation, insoluble protein was removed, and the supernatant was loaded onto a prepared DEAE-Sephacel anion exchange column (10 mM Tris phosphate, pH 7.0). D38E−KSI was eluted with 500 mL of a linear gradient buffer (10−200 mM Tris phosphate, pH 7.0). Fractions were analyzed by UV and SDS−PAGE, and those that contained D38E−KSI were pooled. D38E−KSI was precipitated with solid ammonium sulfate to give ~52% saturation. After the mixture was slowly stirred at 4 °C overnight, the pellet was centrifuged, resuspended in 10 mM potassium phosphate, and dialyzed against several liters of 10 mM potassium phosphate. Purity was assayed by SDS−PAGE to be ~95% or greater. A slight band below D38E−KSI was observed only after overloading the gel ~10 times. Concentration was determined by using the published value for specific activity.[38]

Overall Isomerization of 1 to 3 Catalyzed by an Acetate Ion and Acetic Acid. Acetate-catalyzed isomerization of **1** to **3** was monitored on a Varian Cary 100 biospectrophotometer at 248 nm, at 10−40 °C (λ_{max} for **3** = 248 nm and does not vary significantly over the temperature range studied), and at various concentrations of EDTA (conditions in cuvette: [**1**] ≈ 60 μM, [AcO⁻]/[AcOH] = 0.2−5.7, [AcO⁻ + AcOH] = 0.230−3.00 M, [EDTA] = 0.01, 0.1, 1, 10, or 100 mM, μ = 1.0 M with NaCl, 3.3% MeOH). Progress curves were monitored for ca. 7−10 half-lives. After completion, steroids were extracted three times with chloroform in a 1:1 ratio; the organic layers were pooled, and solvent was removed under vacuum. Product identity was verified on an Agilent 1100 Series, Bruker Esquire 3000 Plus LC/MS, equipped with an APCI source (positive ion mode) using a Beckman Ultrasphere C-18 column with a 45:55 H$_2$O/MeOH mobile phase. Compound **3** and an unidentified side product eluted with retention times of ~7.7 min (m/z = 287), and 3.2 min (m/z = 301), respectively. The identity of **3** was verified by running a known sample in a separate experiment under conditions as described above.

For kinetic experiments, the overall isomerization of **1** by AcOH/AcO⁻ (k_{isom}) was monitored at 13.1−40 °C. Before data collection

(37) Zhao, Q.; Abeygunawardana, C.; Gittis, A. G.; Mildvan, A. S. *Biochemistry* **1997**, *36*, 14616.
(38) Zawrotny, M. E.; Pollack, R. M. *Biochemistry* **1994**, *33*, 13896.
(39) Pollack, R. M.; Zeng, B.; Mack, J. P. G.; Eldin, S. *J. Am. Chem. Soc.* **1989**, *111*, 6419.

(40) Hawkinson, D. C.; Pollack, R. M.; Ambulos, N. P. *Biochemistry* **1994**, *33*, 12172.
(41) Brooks, B.; Benisek, W. F. *Biochem. Biophys. Res. Commun.* **1992**, *184*, 1386.

began, acetate buffers were thermostated at each temperature for at least 15 min and an additional 2 min after addition of **1**, at which point constant temperature was maintained. At each temperature, initial rates were determined from the first 3–4% of the reaction at several substrate concentrations and at least three different total acetate concentrations at three or four pHs (conditions in cuvette: [**1**] ≈ 8–98 μM, [AcO⁻]/[AcOH] = 0.20–5.0, [AcO⁻ + AcOH] = 0.0290–2.91 M, [EDTA] = 10.0 mM, μ = 1.0 M with NaCl, 3.3% MeOH).

Overall Isomerization of 1 to 3 Catalyzed by D38E. Kinetic parameters for the overall isomerization of **1** to **3** by D38E were determined on a Varian Cary 100 biospectrophotometer at 248 nm and ~5–30 °C, in ~5° increments. For a typical experiment, 100 mM potassium phosphate (3.3% MeOH, pH 7.0) was incubated in a thermostated cell for at least 15 min, until the desired temperature was reached, and for an additional 2 min after addition of **1** (final [**1**] ≈ 10–110 μM). Buffer-catalyzed isomerization was monitored for 2 min. D38E-catalyzed isomerization was then initiated by the rapid addition of enzyme (final concentration: [D38E] = 0.50–3.0 μM). The D38E-catalyzed rate of formation of **3** was determined from the first 8–12% of the reaction and was corrected by subtracting the rate of the buffer-catalyzed isomerization. Experiments were performed in triplicate.

Partitioning of 2 by D38E. D38E-catalyzed partitioning was determined as described previously,[38] using a Hi-Tech SF-61 DX2 double-mixing stopped-flow spectrophotometer at or near 243 nm (the isosbestic point for **2**⁻ and **3** varies somewhat with temperature) and at 15.3–39.8 °C in ~5° increments. All of the solutions were thermostated for at least 15 min prior to mixing until the desired temperature was reached. A solution of **1** in 20% MeOH was mixed with 0.5 M NaOH in a 1:1 ratio and was allowed to react for ~0.5 s, thereby generating **2**⁻. The resultant solution was quenched in a 1:5 ratio with a buffered solution of D38E to produce **2** (final conditions in the observation cell: [**2**] ≈ 30 μM, 100 mM phosphate, pH 7.0, 3.3% MeOH, [D38E] = 0.281–1.05 μM). The change in absorbance was monitored until **2** had been completely converted into either **1** or **3**.

Results

Thermodynamic activation parameters for reactions can be determined through an examination of temperature-dependent kinetics, according to the equation

$$\ln(k) = \Delta S^{\ddagger}/R + \ln(k_B T/h) - \Delta H^{\ddagger}/RT \qquad (1)$$

where k is the rate constant, $\Delta S^{\ddagger}$ is the entropy of activation; R is the ideal gas constant, k_B is the Boltzmann constant; T is the temperature in degrees Kelvin; h is Planck's constant, and $\Delta H^{\ddagger}$ is the enthalpy of activation. Over small temperature ranges, a plot of $\ln(k)$ versus $1/T$ is generally linear, yielding a slope that corresponds to the enthalpy of activation. From the intercept of this line, the entropy of activation ($T\Delta S^{\ddagger}$)[42] can be determined. In a similar manner, by measuring equilibrium constants (K) over a range of temperatures, we determined the enthalpies and entropies associated with these equilibria using the van't Hoff equation, $\ln(K) = -\Delta H°/RT + \Delta S°/R$.[43]

Temperature Dependence of the Rate Constant for Overall Isomerization of 1 to 3 by Acetate (k_{isom}). In the course of this work, we found that under some conditions in

---

Table 1. Rate Constants for the Overall Isomerization of **1** to **3** Catalyzed by Acetic Acid and Acetate Ion[a]

T (°C)[b]	$\times 10^5 k_{isom}{}^{HOAc}$ (M⁻¹ s⁻¹)	$\times 10^5 k_{isom}{}^{OAc}$ (M⁻¹ s⁻¹)
13.1	0.83 ± 0.05	1.10 ± 0.08
18.0	1.44 ± 0.09	1.34 ± 0.06
25.0	2.83 ± 0.02	3.09 ± 0.07
30.0	5.45 ± 0.13	5.25 ± 0.12
40.0	12.4 ± 0.2	12.2 ± 0.2

[a] With 10 mM EDTA, 3.3% MeOH, μ = 1.0 M with NaCl. [b] Reported temperatures are ±0.2 °C.

acetic acid/acetate buffer, significant side reactions occur (probably oxidation),[44] thereby giving an observed rate constant that is actually an upper limit of the overall isomerization rate constant. Therefore, we re-evaluated our previous kinetic results[21] by performing the isomerization reactions in the presence of 10 mM EDTA, which substantially reduces or eliminates side product formation.[44] At [EDTA] ≥ 10.0 mM, side product formation is reduced to ≤2% over the temperature range studied. Control experiments with EDTA in water, without acetate buffer, show that EDTA does not significantly catalyze isomerization.

Isomerization of **1** in acetic acid/acetate buffer was monitored by observing the increase in absorbance at 248 nm due to conversion of **1** to **3** (pH = 3.9–5.3, ~13–40 °C). Initial rates were determined from the first 3–4% of the reaction for at least five substrate concentrations. The slope of the initial rate versus substrate concentration plot gives the observed pseudo-first-order rate constant, $k_{isom}{}^{obs}$, at each concentration of buffer (Table S1 in the Supporting Information). For each mole fraction of acetate, $m_f{}^{OAc}$, plots of $k_{isom}{}^{obs}$ versus total buffer concentration ([AcO⁻] + [AcOH]) are linear and give slopes that equal the second-order rate constant, $k_{isom}{}^{pH}$. Y-intercepts of plots of $k_{isom}{}^{pH}$ versus the mole fraction of acetate ion, $m_f{}^{OAc}$, at $m_f{}^{OAc}$ = 0 and $m_f{}^{OAc}$ = 1, yield the second-order rate constants for acetic acid-catalyzed isomerization of **1**, $k_{isom}{}^{HOAc}$, and acetate ion-catalyzed isomerization of **1**, $k_{isom}{}^{OAc}$, respectively (Table 1). Arrhenius plots of ln $k_{isom}{}^{OAc}$ and ln $k_{isom}{}^{HOAc}$ versus $1/T$ are linear and give $\Delta H^{\ddagger}$ = 16.1 ± 1.0 and 17.5 ± 0.6 kcal/mol, respectively, and $T\Delta S^{\ddagger}$ = −7.5 ± 0.8 and −6.1 ± 0.6 kcal/mol, respectively.

The rate constants for acetate ion-catalyzed isomerization, $k_{isom}{}^{OAc}$, in the presence of EDTA agree well with those of our previous work, which was done in the absence of EDTA.[21] However, the rate constants for acetic acid-catalyzed isomerization, $k_{isom}{}^{HOAc}$, while independent of EDTA at temperatures <25.0 °C, are ~2-fold faster in the presence of EDTA than those without it at temperatures >25.0 °C. This results in significantly different values for $\Delta H^{\ddagger}$ and $T\Delta S^{\ddagger}$ for the acetic acid-catalyzed isomerization, $k_{isom}{}^{HOAc}$, by about +4 and −4 kcal/mol, respectively, but with no change in the acetate ion-catalyzed parameters.

Temperature Dependence of the Kinetic Parameters for D38E (k_{cat}/K_M, k_{cat}, and K_M). D38E-catalyzed isomerization of **1** was monitored by observing the increase in absorbance at 248 nm due to conversion of **1** to **3** (at ~5–30 °C). Double reciprocal plots yield the catalytic constants k_{cat}/K_M, k_{cat}, and K_M at each temperature (Table 2). On the basis of the value for

---

(42) Entropy (ΔS), as determined from eq 1, has units of cal/mol K. We report and discuss the entropic contribution to free energy ($T\Delta S$) in kcal/mol for comparison to ΔH and ΔG, which are also reported in kcal/mol. Since $T\Delta S$ is temperature dependent, convention dictates that the activation and equilibrium parameters discussed here be given at 298 K. Thus, a negative value for $T\Delta S$ is considered an entropy loss (unfavorable), while a positive value for $T\Delta S$ is considered an entropy gain (favorable).

(43) The van't Hoff equation used here assumes a standard state of 1 M.

(44) de la Mare, P. B. D.; Wilson, R. D. *J. Chem. Soc., Perkin Trans. 2* **1977**, 157.

**Table 2.** Kinetic Constants for D38E-Catalyzed Isomerization of **1**[a]

T (°C)[b]	$\times 10^{-6}$ k_{cat}/K_M (M^{-1} s^{-1})	k_{cat} (s^{-1})	K_M (μM)
5.4	1.6 ± 0.1	53 ± 1	33 ± 2
10.3	1.9 ± 0.1	71 ± 3	37 ± 3
15.3	2.5 ± 0.1	101 ± 5	40 ± 3
20.1	3.6 ± 0.3	145 ± 8	40 ± 4
25.0	3.3 ± 0.2	180 ± 9	55 ± 3
29.9	4.0 ± 0.2	250 ± 20	63 ± 5

[a] With 100 mM potassium phosphate buffer, pH 7.0, 3.3% MeOH. [b] Reported temperatures are ±0.2 °C.

Table 3. Thermodynamic Parameters for D38E-catalyzed Isomerization of **1** to **3**

kinetic constant	$\Delta G^{\ddagger a}$	$\Delta H^{\ddagger a}$	$T\Delta S^{\ddagger a}$
k_{cat}/K_M	8.5 ± 0.1	5.9 ± 0.8	−2.6 ± 1.0
k_{cat}	14.3 ± 0.1	10.1 ± 0.3	−4.2 ± 0.3
K_M	5.8 ± 0.1	4.3 ± 0.6	−1.5 ± 0.7
k_{isom}^{OAc}	23.5 ± 0.1	16.1 ± 1.0	−7.5 ± 0.8

[a] Values given in kcal/mol at 298 K. Values for K_M are $\Delta G°$, $\Delta H°$, and $T\Delta S°$.

Scheme 4
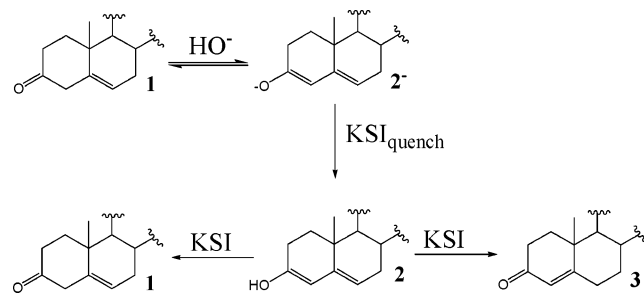
K_M (55 μM at 25.0 °C), the observed activity at 25.0 °C is entirely due to D38E and not to any contaminating wild type. If a small amount of wild-type KSI were present, the K_M determined by these experiments would be identical to that for WT (∼300 μM).[26] Plots of the natural logarithm of the rate constants versus $1/T$ are linear and yield $\Delta H^{\ddagger}$ and $T\Delta S^{\ddagger}$ for D38E catalysis, along with the thermodynamic parameters from the van't Hoff plot for K_M (Table 3).

Temperature Dependence of D38E-Catalyzed Partitioning of 2. Partitioning of the intermediate (**2**) by D38E was monitored by the sequential-mixing stopped-flow method, as previously described.[38] Dienolate (**2**$^-$) was formed by rapidly mixing a solution of **1** with 0.5 M NaOH for ∼0.5 s. When this solution is quenched with a buffered solution of D38E, **2**$^-$ is protonated to give **2**, which then partitions to **1** and **3** (Scheme 4). The variation in UV absorbance was monitored at the isosbestic point for **2** and **3** and follows the general trend of previous data.[39] An initial rapid decrease, which is the result of the partitioning of **2** to **1** (k_{-1}^{D38E}) and **2** to **3** (k_2^{D38E}) by D38E, is followed by a subsequent slower increase in absorbance, resulting from conversion of **1** to **3** (k_{cat}/K_M).

These kinetic traces were fit to the reaction mechanism (Scheme 5) using the KINSIM/FITSIM program.[45] The diffusion rate constant, k_{on}^2, was calculated[46] for each temperature and was not allowed to vary throughout fitting. The calculated rate constants for the overall isomerization (k_{cat}/K_M) are not reported in Table 4 because the time scale required to monitor partitioning is too short to observe significant isomerization. However, fits

Scheme 5
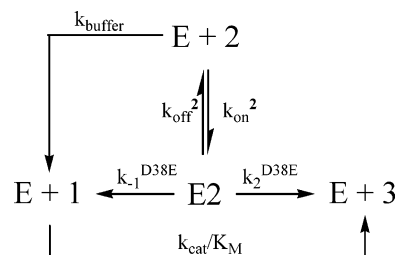
Table 4. Rate Constants[a] for D38E-Catalyzed Partitioning of **2**$^-$ [b]

T (°C)[c]	k_{off}^2 (s^{-1})[d]	k_{-1}^{D38E} (s^{-1})[e]	k_2^{D38E} (s^{-1})[e]
15.3	800	210	230
20.2	1100	290	340
25.4	1800	480	570
30.4	2900	780	910
35.2	4000	1060	1410
39.8	5000	1390	1930

[a] Values are an average of at least six individual trials. [b] With 100 mM potassium phosphate buffer, pH 7.0, 3.3% MeOH. [c] Reported temperatures are ±0.2 °C. [d] Error is ∼100%. [e] Error is ∼20%.

Table 5. Summary of the Rate and Equilibrium Constants for Isomerization of **1** to **3** Catalyzed by D38E[a] and Acetate Ion[b]

reaction	constant	$\Delta G^{c,d}$ (kcal/mol)	ΔH^c (kcal/mol)	$T\Delta S^{c,d}$ (kcal/mol)
E1 ⇌ E + 1	K_S	5.8 ± 0.1	4.3 ± 0.6	−1.5 ± 0.7
E1 → TS1	k_1^{D38E}	13.9 ± 0.1	7.6 ± 0.1	−6.3 ± 0.1
E2 → TS1	k_{-1}^{D38E}	13.8 ± 0.1	13.9 ± 0.5	0.0 ± 0.5
E2 → TS2	k_2^{D38E}	13.7 ± 0.1	15.5 ± 0.3	1.8 ± 0.3
E1 ⇌ E2	K_{int}	0.0 ± 0.1	−6.3 ± 0.5	−6.3 ± 0.5
E + 1 → TS1	k_1^{D38E}/K_S	8.1 ± 0.1	3.3 ± 0.7	−4.8 ± 0.8
AcO$^-$ + 1 → TS1^{Ac}	k_1^{OAc}	21.4 ± 0.1	16.4 ± 1.9	−5 ± 2
AcOH + 2$^-$ → TS1^{Ac}	k_{-1}^{OAc}	10.3 ± 0.1	9.6 ± 1.8	−0.7 ± 0.3
AcOH + 2$^-$ → TS2^{Ac}	k_2^{HOAc}	12.5 ± 0.1	8.4 ± 0.6	−4.2 ± 0.7
AcO$^-$ + 1 ⇌ AcOH + 2$^-$	K_{eq}^1	11.1 ± 0.1	7 ± 2	−4 ± 2

[a] From the present work. [b] From previous work (ref 21). [c] Reported values of ΔG, ΔH, and $T\Delta S$ are activation ($\ddagger$) parameters for rate constants. For the equilibrium constants, values for ΔG, ΔH, and $T\Delta S$ correspond to that for a standard state (degree) of 1 M. [d] Values are given at 298 K.

to Scheme 5 did give values for k_{cat}/K_M that are within ∼20% of the actual values determined from initial rate experiments. The rate constants[49] k_{off}, k_{-1}^{D38E}, and k_2^{D38E} at each temperature are given in Table 4. Both k_{-1}^{D38E} and k_2^{D38E} increase with increasing temperature, and linear Arrhenius plots give values for the enthalpy and entropy of activation for both protonation steps (Table 5). Additionally, the thermodynamic activation parameters for D38E-catalyzed proton abstraction from C-4 ($\Delta H^{\ddagger}$ and $T\Delta S^{\ddagger}$ for k_1^{D38E}) can be calculated from these rate constants, based on analysis of Scheme 2, by the net rate constant approximation[50] and the assumption that k_2^{D38E} is irreversible (i.e., $k_{-2}^{D38E} \ll k_2^{D38E}$), using the following equation: $k_1^{D38E} = k_{cat}(k_2^{D38E} + k_{-1}^{D38E})/(k_2^{D38E} - k_{cat})$. These values are also given in Table 5.

Discussion

The often dramatic reduction in free energy for an enzymatic reaction is typically discussed in terms of the enzyme's ability to stabilize the bound transition state(s) relative to that of the transition state(s) in solution.[10] However, an analysis of enzymatic thermodynamic activation parameters can enable a more detailed discussion of the mechanism(s) of stabilization of the transition state(s) than a consideration of free energies

alone. Enthalpic stabilization generally results from favorable polar and electrostatic interactions between enzyme and the transition state, whereas entropic stabilization can be attributed to changes in conformation or to changes in solvation. Jencks has argued that enzymes catalyze reactions primarily by making entropic changes from an enzyme—substrate complex to products more favorable than in solution.[7] Jencks reasoned that, in a bimolecular reaction between A and B in solution, decreases in entropy result from losses of both translational and rotational freedom.[7] He maintained that enzymes overcome unfavorable entropy by bringing A and B together in the active site so that once bound, the entropy change from ground state to transition state is minimal or even positive. Thus, the conversion of the enzyme—substrate complex to products (k_{cat}) often shows a more-favorable entropy than that of the corresponding non-enzymatic reaction in aqueous solution. For example, k_{cat} for cytidine deaminase-catalyzed deamination of 5,6-dihydro-cytidine is ~8 kcal/mol entropically more favorable than the spontaneous first-order reaction.[18] The favorable entropy is attributed to changes in the active-site hydration and conformation of a glutamate residue.[18] Warshel,[13] however, has argued that the Jencks' rationale overestimates the contribution of entropy to catalysis.

In a recent review by Wolfenden,[51] the catalytic power (k_{cat}/K_M) of single substrate enzymes is attributed to their ability to lower $\Delta H^{\ddagger}$, while effecting minimal changes in $\Delta S^{\ddagger}$, relative to an uncatalyzed reaction in aqueous solution. He concluded that the affinity of a transition state for an enzyme is due to predominantly electrostatic interactions, including hydrogen bonds, that act in concert with one another. Indeed, these interactions are necessary in a variety of enzymatic reactions, such as deamination of cytidine by cytidine deaminase,[17] racemization of mandelate by mandelate racemase,[19] and hydrolysis of cytidine cyclic 2′,3′-phosphate by ribonuclease A.[16] For example, deamination of cytidine by cytidine deaminase is characterized by $\Delta H^{\ddagger}_{k_{cat}/K_M} = 2$ kcal/mol, whereas in solution, $\Delta H^{\ddagger}_{k_{non}} \approx 22$ kcal/mol, corresponding to a reduction in activation enthalpy of ~20 kcal/mol.[17] A significant portion of this enthalpic stabilization results from the interaction between the 2′-OH of the ribose ring of cytidine and Glu91 of cytidine deaminase, as shown by an increase of $\Delta H^{\ddagger}_{k_{cat}/K_M}$ to ~10 kcal/mol in the E91A mutant.[17] This difference corresponds to a $\Delta\Delta H^{\ddagger}$ of 8 kcal/mol, which can be attributed to the hydrogen bonding interaction between Glu91 and 2′-OH of the ribose ring of cytidine.

(45) Dang, Q.; Frieden, C. *Trends Biochem. Sci.* **1997**, *22*, 317.
(46) The rate constant for diffusion of **2** and D38E to form the **E2** complex, k_{on}^2, was calculated at each temperature using the equation $k_{on}^2 = (2RT/30\,000) \times ((r_2 + r_E)^2/r_2 r_E)$,[47] where *R* is the ideal gas constant, and *T* is the temperature; η is the viscosity of the solvent at each temperature,[48] and r_2 and r_E are the radii of **2** and KSI, respectively. The radii, r_2 and r_E, were estimated by measuring the widest diameter of each molecule using Rasmol, version 2.7.1, from the crystal structure of the KSI—equilenin complex determined by Cho et al. (PDB ID: 1QJG).[30]
(47) Connors, K. A. *Chemical Kinetics: The Study of Reaction Rates in Solution*; VCH Publishers: New York, 1990; p 134.
(48) *CRC Handbook of Chemistry and Physics*, 55th ed.; Weast, R. C., Ed.; CRC Press: Ohio, 1974; p F-49.
(49) Values of k_{off}^2 are very sensitive to fixed values of k_{cat}/K_M, and so k_{cat}/K_M was allowed to vary during fitting. Because of this, the values reported in Table 4 for k_{off}^2 have an error of ~100%. Additionally, the values for k_{off}^2 reported here are ~1 order of magnitude greater than our previous determinations,[38] which is due to the inaccuracy of this method to determine k_{off}^2. Values of k_{-1}^{D38E} and k_2^{D38E} are only slightly sensitive to k_{off}^2 values, and we estimate ~20% error in these reported rate constants.
(50) Cleland, W. W. *Biochemistry* **1975**, *14*, 3220.
(51) Wolfenden, R. *Biophys. Chem.* **2003**, *105*, 559.

In many cases, both $T\Delta S^{\ddagger}$ and $\Delta H^{\ddagger}$ for the enzymatic reaction are more favorable than those for the nonenzymatic reaction,[16−19] although there are exceptions to this trend.[15] It is generally thought that the majority of entropy loss for a nonenzymatic reaction results from bringing two or more molecules together, and the entropy changes from the bond making/bond breaking steps of catalysis are minimal.[7] The typically large enthalpic costs due to bond making/bond breaking can be overcome by an enzyme's ability to provide favorable ionic and hydrogen bonding interactions that are not available in solution.[14]

Complicating the interpretation of differences in activation parameters between enzymatic and nonenzymatic reactions is the fact the there are often several steps that contribute to the overall enzymatic rate constant, including binding, product release, and chemical steps. Similarly, observed nonenzymatic rate constants are generally a combination of individual steps, each with a distinct transition state. Although the activation parameters for the overall rate constants of both enzymatic and nonenzymatic reactions have been determined in many cases, we are unaware of any previous studies that have examined these parameters for the microscopic rate constants of both enzymatic and nonenzymatic reactions. Additionally, enzymatic reactions are often compared to nonenzymatic reactions in moderately dilute buffer, which may not provide the best model for the enzymatic mechanism. While these comparisons are useful, the ability to determine differences in the detailed transition-state interactions requires a comparison of an enzymatic reaction to a specific nonenzymatic reaction catalyzed by an appropriate model compound. KSI provides an excellent system to do just that by a comparison of the activation parameters of the microscopic rate constants for D38E to the activation parameters of the acetate ion-catalyzed isomerization.[21]

Relative to the nonenzymatic, acetate ion-catalyzed reaction (k_{isom}^{OAc}),[21] D38E lowers the activation enthalpy for k_{cat}/K_M by about 10 kcal/mol and raises the activation entropy by about 5 kcal/mol for the overall isomerization (Table 3). The reaction mechanisms for both acetate- and D38E-catalyzed isomerization have been extensively characterized, and there are several steps that contribute to the overall isomerization rates. To make useful comparisons, it is first necessary to consider the individual chemical and binding steps for both reactions.

Substrate Binding by D38E ($K_M \approx K_S$). Because $k_1^{D38E} \ll k_{off}^1$ for the D38E mutant of KSI, K_M may be equated to K_S, the dissociation constant for the **E1** complex.[38] The enthalpy and entropy for dissociation of the **E1** complex (K_M) are given in Table 3. Because the sign and magnitude of binding entropy are dependent on the choice of standard state, we limit the discussion of K_S to ΔH°. The favorable enthalpy of binding ($\Delta H^{\circ} = -4.3$ kcal/mol) may result from the difference in the relative strength of the hydrogen bonds made in the **E1** complex and in the free species **E** + **1** (Scheme 6, path a). Hydrogen bonds in the **E1** complex are stronger than those in **E** + **1**. Both experimental and computational determinations of the enthalpy of a hydrogen bond in water give estimates of ~2−4 kcal/mol.[52,53] Increased hydrogen bond strength in even moderately hydrophobic active sites relative to solution is not

(52) Li, Z.; Lazaridis, T. *J. Am. Chem. Soc.* **2003**, *125*, 6636.
(53) Patil, K. J.; Pawar, R. B. *Spectrochim. Acta, Part A* **2003**, *59*, 1289.

Scheme 6

uncommon.[54,55] Yoshida et al.[56] measured the hydrogen bond strength between phenol and various ketones in CCl_4 as a model for the interior of a protein. They found that the enthalpy of hydrogen bond formation between phenol and 2-butanone in CCl_4 is 5.8 kcal/mol, $\sim$2 kcal/mol stronger than that of the hydrogen bond in aqueous solution.[56] Thus, the favorable enthalpy for association of **1** and D38E can be attributed to the stronger hydrogen bonding interaction in the active site relative to that in aqueous solution.

D38E-Catalyzed Proton Abstraction from C-4 of 1 (k_1^{D38E}). Proton abstraction from C-4 of **1** by Glu38 results in an unfavorable entropy term ($T\Delta S^{\ddagger} = -6.3$ kcal/mol) and a moderate enthalpy term ($\Delta H^{\ddagger} = +7.6$ kcal/mol). There are two main processes occurring at **TS1**: (1) proton transfer between **1** and Glu38 and (2) strengthening of the hydrogen bonds between O-3 of **1** and both Asp99 and Try14 (Scheme 6, path b). Partial bond formation restricts rotation of the carboxylate of Glu38, resulting in a loss of entropy relative to the ground state, which can be estimated as 0–5 kcal/mol.[7,57] Changes in conformation resulting from tightening of hydrogen bonds at the transition state generally result in an entropic cost of $\sim$3–7

kcal/mol per bond.[7] The overall negative entropy (-6.3 kcal/mol), associated with k_1^{D38E}, is consistent with these estimates and suggests that the active site is constricting as the hydrogen bonds between D38E and **1** become stronger.

Proton abstraction by an acetate ion from **1** has an enthalpy of activation of 16.4 kcal/mol,[21] which is similar to the enthalpies of activation of $\sim$15–30 kcal/mol[58,59] typically observed for proton abstractions from carbon atoms α to a carbonyl. In the active site of KSI, $\Delta H^{\ddagger}$ is reduced by $\sim$9 kcal/mol, equivalent to a rate increase of $\sim$10^6-fold. The much more favorable enthalpy for proton transfer in the enzyme active site (k_1^{D38E}) may be due to the increased strengthening of the hydrogen bonds between Asp99 and Tyr14 and steroid as the reaction progresses. The developing charge on O-3 at **TS1** results in stronger hydrogen bonds at O-3 relative to the neutral O-3 in the ground state since hydrogen bonds involving neutral atoms are generally weaker than hydrogen bonds involving charged atoms.[60] In addition, the active site of KSI provides a

(54) Avbelj, F.; Baldwin, R. L. *Proc. Natl. Acad. Sci. U.S.A.* **2003**, *100*, 5742.
(55) Shan, S.-O.; Herschlag, D. *Proc. Natl. Acad. Sci. U.S.A.* **1996**, *93*, 14474.
(56) Yoshida, Z.; Ishibe, N. *Spectrochim. Acta, Part A* **1968**, *24*, 893.

(57) Colonna, G.; Di Masi, N. G.; Marzilli, L. G.; Natile, G. *Inorg. Chem.* **2003**, *42*, 997.
(58) Chiang, Y.; Kresge, A. J.; Schepp, N. P. *J. Am. Chem. Soc.* **1989**, *111*, 3977.
(59) Casale, J. F.; Lewin, A. H.; Bowen, J. P.; Carroll, F. I. *J. Org. Chem.* **1992**, *57*, 4906.
(60) Shan, S.-O.; Herschlag, D. *J. Am. Chem. Soc.* **1996**, *118*, 5515.

hydrophobic environment in which a hydrogen bond can be strengthened substantially more than in an aqueous environment.[55]

Partitioning of 2⁻ by D38E (k_{-1}^{D38E} and k_2^{D38E}). D38E partitions the intermediate almost equally to product and substrate, and this ratio, defined as k_2^{D38E}/k_{-1}^{D38E}, is 1.2 at 25.0 °C, which is in good agreement with our previous results.[38] Despite the error in these measurements (~20%), there is a significant temperature dependence of the partitioning over the temperature range studied here. The activation parameters for both k_{-1}^{D38E} and k_2^{D38E} are largely enthalpic, with little to no changes in entropy (Table 5). At both **TS1** and **TS2**, partial bond formation restricts rotational and vibrational freedom of the active site base (Glu38) and the rotational and vibrational freedom of the steroid (Scheme 6, paths c and d). Although the $\Delta G^{\ddagger}$ values for formation of **TS1** (k_{-1}^{D38E}) and **TS2** (k_2^{D38E}) are the same, $\Delta H^{\ddagger}$ for k_{-1}^{D38E} is ~2 kcal/mol more favorable than for k_2^{D38E}, while $T\Delta S^{\ddagger}$ is more favorable for k_2^{D38E} than for k_{-1}^{D38E} by the same amount. Thus, the equal free energies of these two transition states are due to compensating differences in $\Delta H^{\ddagger}$ and $T\Delta S^{\ddagger}$.

A plausible explanation for this difference comes from a consideration of hydration differences of the active site at the two transition states (**TS1** and **TS2**). Molecular dynamics simulations of **E1** indicate the presence of water, while there is none in the simulated **E2** complex.[35] Thus, during the conversion of **E1** to **E2** (k_1^{D38E}), water is released from the active site, and the reaction of **E2** to **E1** (k_{-1}^{D38E}) involves the re-entry of water into the active site. The entropy gain for release of a water molecule from an active site is ~2–3 kcal/mol,[61,62] which suggests that water entering the active site should result in an entropic *loss* of ~2–3 kcal/mol for k_{-1}^{D38E}. Additionally, Feierberg and Åqvist[33] simulated the entire reaction coordinate of KSI-catalyzed isomerization of **1** to **3** with and without a water molecule present in the active site. They found that the free energy change for the **E2** to **E3** conversion (k_2^{D38E}) is best simulated when no water molecule is present in the active site in either **E2** or **E3**. Thus, for k_{-1}^{D38E}, there is an entropic cost due to water re-entering the active site at **TS1**, but there is no such penalty in k_2^{D38E} (**TS2**), leading to a more entropically favorable **TS2** by ~2 kcal/mol, relative to **TS1**.

The enthalpies of activation for both k_{-1}^{D38E} and k_2^{D38E} are unfavorable ($\Delta H^{\ddagger} = 13.9$ and 15.5 kcal/mol, respectively). Proton transfer from Glu38 to the steroid and weakening of the hydrogen bonds between steroid and Asp99/Tyr14 contribute to a large, positive enthalpy of activation for both steps. The difference in enthalpy of the two transition states (**TS1** and **TS2**) ($\Delta H^{\ddagger} = -1.8$ kcal/mol) may arise from differences in hydration. An additional water molecule present in **TS1** could result in polar interactions that are not present in **TS2**, resulting in the small reduction in enthalpy for k_{-1}^{D38E} compared to k_2^{D38E}.

The Keto–Enolate Equilibrium Constant (K_{int}). The internal equilibrium constant between **E1** and **E2** (K_{int}) can be calculated directly from the ratio k_1^{D38E}/k_{-1}^{D38E}. At 25.4 °C, $K_{int} = 0.9$, which is in good agreement with the previous estimate of 1.3 at 25.0 °C.[38] The changes in enthalpy and entropy (ΔH and $T\Delta S$) for this equilibrium, which were determined from the temperature dependence of K_{int}, are −6.3 and −6.3 kcal/

mol, respectively. The negative dienolate is stabilized enthalpically by the formation of hydrogen bonds between O-3 of **2⁻** and both Asp99 and Tyr14 (Scheme 6, path e). These hydrogen bonds are expected to be stronger with the oxanion of **2⁻** than with the neutral carbonyl oxygen of **1**, resulting in a favorable enthalpy.[60] Calculations by Mazumder et al.[35] showed that for wild-type KSI, the **E2** complex is more constricted than **E1**, and the negative entropy for this equilibrium is likely a result of this more-rigid **E2** complex. The equilibrium between **E1** and **E2** is entropically costly, but this cost is offset by the enthalpic gain of the hydrogen bonds to the oxanion, resulting in K_{int} near unity ($\Delta G \approx 0$ kcal/mol).

Comparison to the Acetate-Catalyzed Isomerization. A summary of the activation and equilibrium parameters for both D38E- and acetate ion-catalyzed isomerization of **1** to **3** is given in Table 5, and diagrams based on this and previous work[21] are shown in Figure 2. The major differences between the free energy ($\Delta G^{\ddagger}$) diagrams of acetate ion and D38E catalyses are (1) that D38E equalizes the energies of bound substrate and bound intermediate (dienolate), whereas in solution, the intermediate (**2⁻**) is ~11 kcal/mol higher in free energy and (2) that D38E lowers and equalizes the free energies of **TS1** and **TS2**, whereas in solution, the free energy of **TS2^{Ac}** is greater than that of **TS1^{Ac}** by ~2 kcal/mol. The overall catalytic effect of D38E then can be attributed to a reduction of the free energy of the intermediate and the flanking transition states and to selective stabilization of the second chemical transition state, relative to the first.

Determination of the activation parameters for both acetate and D38E enables a dissection of the free energy diagrams into their enthalpic and entropic components. Figure 2 (parts B and C) illustrates the enthalpy (ΔH) and entropy ($-T\Delta S$) changes, respectively, that occur during the isomerization reactions. As shown in panel A, an increase in enthalpy (ΔH), which causes a decrease in rate, is depicted as an increase in the y-axis of Figure 2B. Similarly, in Figure 2C, an increase in $-T\Delta S$ (or decrease in entropy) is shown as an increase in the y-axis.

Equilibrium between 1 and 2⁻. One common enzymatic strategy is to lower the free energy of highly reactive intermediates relative to reactants and products. For reversible enzymes at equilibrium (i.e., enzymes that are not under metabolic control), "catalytic perfection" predicts that a bound intermediate should have about the same free energy as would the bound substrate and bound product.[63] Consistent with this expectation, the bound high-energy dienolate intermediate of KSI (and D38E) is stabilized to give an internal equilibrium constant between **E1** and **E2** of about unity. For D38E, this internal equilibrium constant results from a compensating favorable enthalpy ($\Delta H° = -6.3$ kcal/mol) and an unfavorable entropy ($T\Delta S° = -6.3$ kcal/mol) (Figure 2, B and C, black trace). In solution, however, the relative free energy for the intermediates (**2⁻** + AcOH) is significantly greater than that of reactants (**1** + AcO⁻) ($\Delta G° = 11$ kcal/mol, Figure 2A, red trace), due to both an unfavorable enthalpy ($\Delta H° = +7$ kcal/mol) and an unfavorable entropy ($T\Delta S° = -4$ kcal/mol) (Figure 2, B and C, red trace). Thus, the more-favorable equilibrium at the active site of D38E is due almost entirely to more favorable enthalpic effects for the enzyme than that for the acetate ($\Delta\Delta H° \approx 13$ kcal/mol), with entropy differences playing only a minor role. These results are

(61) Dunitz, J. D. *Science* **1994**, *264*, 670.
(62) Suresh, S. J.; Naik, V. M. *J. Chem. Phys.* **2000**, *113*, 9727.

(63) Albery, J. W.; Knowles, J. R. *Biochemistry* **1976**, *15*, 5631.
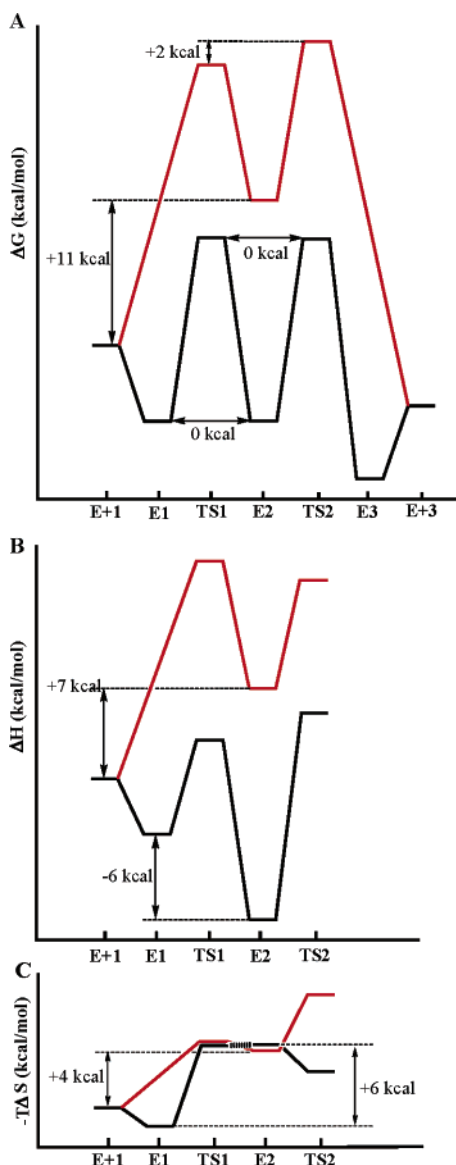
Figure 2. Reaction coordinates for D38E- (−, black) and acetate ion (−, red)-catalyzed isomerization of **1** to **3**. (A) Gibbs free energy diagram, (B) enthalpy diagram, and (C) entropy diagram. To aid in the direct comparison of A and B, entropy units are given as $-T\Delta S$. When reading the figure, the reader should keep in mind that an increase in $-T\Delta S$ is unfavorable and a decrease in $-T\Delta S$ is favorable. Thermodynamic parameters correspond to data at 25.0 °C, and these values are listed in Table 5. The *x*-axis corresponds to the reaction coordinate for D38E-catalyzed isomerization. The corresponding acetate ion-catalyzed mechanism is $AcO^- + \mathbf{1} \rightleftharpoons \mathbf{TS1^{Ac}} \rightleftharpoons AcOH + \mathbf{2^-} \rightleftharpoons \mathbf{TS2^{Ac}} \rightleftharpoons AcO^- + \mathbf{3}$. Barriers due to $\mathbf{E} + \mathbf{1}$ association/dissociation and barriers due to acetate-catalyzed rate constants assume a standard state of 1 M.

consistent with previous work that attributes the major driving force for stabilization of the bound intermediate to hydrogen bonds from Asp99 and Tyr14 to O-3 of $\mathbf{2^-}$ in the hydrophobic active site of KSI.[28,30,32,33]

Proton Abstraction from 1. The second-order rate constant for proton abstraction catalyzed by D38E ($\mathbf{E} + \mathbf{1} \rightarrow \mathbf{TS1}$, k_1^{D38E}/K_S) can be compared to the second-order rate constant for acetate-catalyzed proton abstraction ($AcO^- + \mathbf{1} \rightarrow \mathbf{TS1^{Ac}}$, k_1^{OAc}) (Table 5 and Scheme 6, path f). Proton abstraction from C-4 by an acetate ion has a large enthalpic penalty and a moderate entropic penalty (Figure 2, B and C, red trace). D38E lowers the enthalpy of activation, but has no effect on the entropy of

activation for this step ($\Delta\Delta H^{\ddagger}_{k_1} = \Delta H^{\ddagger}_{k_1^{D38E}/K_M} - \Delta H^{\ddagger}_{k_1^{OAc}} = 13$ kcal/mol, $T\Delta\Delta S^{\ddagger}_{k_1} = 0$ kcal/mol; Table 5). As discussed previously, the strength of a hydrogen bond in a hydrophobic active site is much greater than one in aqueous solution.[55] Thus, the binding of **1** to D38E ($1/K_S$) results in enthalpically favorable hydrogen bonding interactions relative to those in solution ($\Delta H° = -4.3$ kcal/mol). Additionally, the increase in hydrogen bond strength as charge is formed on O-3 of **1** is expected to be greater in a hydrophobic environment than in the aqueous environment of acetate buffer,[55] resulting in a reduction of enthalpy for proton abstraction ($\Delta\Delta H^{\ddagger}_{k_1}$). Thus, the decrease in free energy for proton abstraction by D38E relative to that of acetate ($\Delta\Delta G^{\ddagger}_{k_1} = \Delta G^{\ddagger}_{k_1^{D38E}/K_M} - \Delta G^{\ddagger}_{k_1^{OAc}} = -13$ kcal/mol) is consistent with favorable hydrogen bonding interactions provided by the active site that are not present in an aqueous environment.

Partitioning of the Intermediate ($\mathbf{2^-}$). The free energy barrier for acetic acid-catalyzed protonation at C-4 of $\mathbf{2^-}$ is ∼2 kcal/mol lower than that for the protonation at C-6 (Figure 2A, red trace). Thus, ∼98% of the time, $\mathbf{2^-}$ reverts back to substrate rather than forming product. From a catalytic perspective, the reprotonation at C-4 is a lost opportunity. Consistent with the expectation for a "perfect" enzyme,[63] partitioning of the intermediate at the active site of KSI results in a roughly 1:1 mixture of products and reactants. Similarly, D38E selectively stabilizes **TS2** over **TS1**, leading to nearly isoenergetic transition states (Figure 2A, black trace). We have previously postulated a mechanistic rationale for this change in the partitioning of the intermediate at the active site in terms of differences in hydrogen bond strengths.[32] We suggested that differences in conformations of the A-ring of the steroids in the transition states might result in stronger hydrogen bonds from Asp99 and Tyr14 to O-3 at **TS2** than at **TS1**. In the present work, we find that there is an entropic contribution to the partitioning. A comparison of entropies of activation reveals that k_{-1}^{HOAc} is entropically favored over k_2^{HOAc} ($T\Delta\Delta S^{\ddagger}_{k_{-1}-k_2} = 3.5 \pm 1.0$ kcal/mol) in the acetate ion-catalyzed reaction, but entropy favors k_2^{D38E} ($T\Delta\Delta S^{\ddagger}_{k_{-1}-k_2} = 1.8 \pm 0.8$ kcal/mol) in the enzymatic reaction (Figure 2). As discussed above, these changes in the partitioning of the intermediate at the enzyme active site may be influenced by changes in hydration between **TS1** and **TS2**. In the conversion of **E2** to **TS1**, water re-enters the active site, resulting in a loss of entropy for this step relative to that for the conversion of **E2** to **TS2**, which does not involve a hydration change, resulting in a selective reduction of the activation barrier for k_2^{D38E}, relative to k_{-1}^{D38E}.

Summary and Conclusions

Isomerization of **1** to **3** occurs 13 orders of magnitude faster when catalyzed by KSI than when catalyzed by an acetate ion. Determination of the activation parameters for the microscopic rate constants for both the D38E- and the acetate ion-catalyzed isomerization has allowed further characterization of the basis for this catalysis. Enzymatic stabilization of the intermediate dienolate relative to the substrate is due entirely to favorable enthalpic interactions at the active site of KSI, which are not available in solution, consistent with an increased hydrogen bonding ability of the enzyme. Similarly, the more-favorable enthalpy of activation for k_1^{D38E}/K_S relative to that for k_1^{OAc} for proton abstraction from C-4 of **1** indicates that the enzymatic acceleration of this process is due to the ability of KSI to make hydrogen bonding interactions in the active site stronger than

those available in solution. Partitioning of the intermediate, however, has a substantial entropic component, suggesting that equalization of the two high-energy transition states of KSI, **TS1**, and **TS2** may be affected by hydration changes in the active site.

Supporting Information Available: A table of k_{isom}^{obs} at various temperatures. This information is available free of charge via the Internet at http://pubs.acs.org.

JA046819K